Direct measurements of vapor pressures of chlorinated paraffin congeners from technical mixtures

Jort Hammer[*], Hidenori Matsukami, Hidetoshi Kuramochi, Satoshi Endo[*]

National Institute for Environmental Studies (NIES), Tsukuba, Ibaraki, Japan

E-mail contact: hammer.jort@nies.go.jp, endo.satoshi@nies.go.jp

ABSTRACT

Chlorinated Paraffins (CPs) are a complex group of manmade chemicals detected widely in the environment. To predict their environmental fate and effects, it is important to understand their physical-chemical properties including vapor pressure. In this study, the first direct measurements of the vapor pressure for CP congener groups ($C_{10-16}Cl_{4-11}$) are presented. Vapor pressure was measured above three industrial CP mixtures with different congener distributions between 20 and 50°C using a gas saturation method. The measured saturated vapor pressure (P^*) decreased with increasing carbon chain length and Cl content. ΔH_{vap} ranged between 73 and 122 kJ mol^{-1}, consistent with data from the literature and model prediction. The experimental log P^* at 25°C agreed well with predictions from an empirical regression model in the literature ($R^2 = 0.97$; RSME = 0.25) and with those predicted from the COSMO-RS-trained fragment contribution model ($R^2 = 0.95$; RSME = 0.35). A new empirical model was calibrated with the P^* data for 35 congener groups measured in this study. Predicted log P^* values correlate well with field-measured

22   gas/particle partition coefficients and may therefore be used for estimating the

23   environmental fate and pathways of a broad range of CPs in the environment.

24

25   **Keywords:** Gas Saturation, Congener groups, Enthalpy of vaporization, SCCP, MCCP,

26   COSMO-RS

INTRODUCTION

Chlorinated Paraffins (CPs) are a group of high-volume production chemicals and are widely used for their thermal and chemical stability. CPs are applied in various products as, e.g., plasticizers, coolants, and flame retardants. Because of their widespread use, CPs are regularly released into the environment during production, transportation, and recycling processes and through leaching and volatilization from landfills (Tomy et al. 1998; Sverko et al. 2012; Brandsma et al. 2019). In 2017, short-chain chlorinated paraffins (SCCPs; C_{10}-C_{13}) were classified as persistent organic pollutants (POPs) under the Stockholm Convention (United Nations Environment Programme (UNEP) 2017). The production of SCCPs has therefore stopped in, e.g., Europe, the US and Japan. However, SCCPs are still ubiquitous in waste (Matsukami and Kajiwara 2019; Matsukami et al. 2020) and have been detected in most environmental compartments including ambient air (Fridén et al. 2011; Huang et al. 2017; van Mourik et al. 2020). Moreover, other CPs (i.e., medium-chain CPs (MCCPs, C_{14}-C_{17}) and long-chain CPs (LCCPs, C_{18} and longer)) are still being produced and used (Brandsma et al. 2017). It is therefore imperative to conduct environmental risk assessments of CPs based on sound scientific understanding of their environmental behavior.

Physicochemical properties such as partition coefficients and vapor pressure are used to understand transport and environmental fate of pollutants. Congener-specific data for such properties would be desirable to capture the varying occurrence of CP congeners, although there is little experimental data available now. In the literature, indirect measurements of the octanol/water partition coefficient and the saturated vapor pressure using

3

49   chromatographic retention approaches have been reported (Drouillard et al. 1998; Hilger et

50   al. 2011). Additionally, various computational methods have been explored to estimate the

51   properties of CP congeners (Glüge et al. 2013). In previous studies, we also have

52   investigated congener-specific partition properties of CPs using GC retention indices and

53   quantum chemically based calculations (Endo and Hammer 2020; Hammer et al. 2020).

54   While such experimental and computational estimations are useful and may be best

55   attainable for a majority of components in a complex mixture, there also is a strong need

56   for direct experimental data to back up the reliability of such estimations.

57   The objective of this work was to determine vapor pressures of CPs on a homologue

58   basis (i.e., a group of congeners with the same molecular formula). Vapor pressure of a

59   chemical is considered a surrogate property for chemical's volatility in the environment. A

60   gas saturation method with a generator column was used to measure the partial vapor

61   pressure (P) of each congener group above CP technical mixture between 20 and 50°C.

62   Three technical mixtures were selected based on differing congener distributions so that the

63   vapor pressures of a range of CP congeners could be investigated. The measured P was

64   used to obtain the saturated vapor pressure (P^*) for each congener group, assuming an ideal

65   mixture. This study provides the first direct measurements of the congener group-specific

66   vapor pressures for CPs, which allows development and evaluation of P and P^* prediction

67   methods.

68

69

70

4

MATERIALS AND METHODS

Chemicals and CP mixtures

Acetone (pesticide and polychlorinated biphenyl analysis grade 5000), methanol

(LC/MS grade) and ammonium acetate (Japan Industrial Standard special grade) were

purchased from FUJIFILM Wako Pure Chemical Corporation (Osaka, Japan). Two

commercial technical CP mixtures, Paroil 179-HV and Chlorowax 500C were provided by

AccuStandard Inc. (New Haven, CT, USA). Another technical mixture was provided by

Shandong Yousuo Chemical Technology Co., Ltd. (China) (Nishida et al. 2019), and is

hereby referred to as the SYCT-wax mixture. The distributions of CP congeners in these

mixtures were determined by liquid chromatography-electrospray ionization-tandem mass

spectrometry (LC-ESI-MSMS) (Matsukami et al. 2020; McGrath et al. 2021), as described

below.

Gas saturation method

The gas saturation method used in this study is similar to the methods presented by

Widegren and Bruno (2010) and Kuramochi et al. (2014). Briefly, nitrogen carrier gas was

passed through a generator column containing CP mixture. The equilibrated vapor was

trapped at the outlet of column and analyzed for concentrations of CP congener groups.

More details are explained in the following.

The generator column consisted of 2 m polytetrafluoroethylene (PTFE) tubing (6.35

mm o.d., 4.35 mm i.d., GL Sciences, Japan) filled with solvent-cleaned borosilicate glass

beads (3 mm in diameter, AS ONE, Japan). Approximately 150–400 mg of CP mixture was

5

93 diluted with 5 mL of acetone and was pipetted into the glass beads-filled PTFE tube.

94 Acetone was then slowly evaporated under a nitrogen flow, leaving the beads coated with

95 CP mixture. During evaporation, the column was moved occasionally so that the remaining

96 solution of CP mixture was re-distributed within the column to achieve even distribution. A

97 1/8" stainless-steel tube (2.2 mm i.d. × 3.0 m in length, GL Sciences) was connected to the

98 inlet of the generator column as a pre-heating column. The generator column was placed in

99 a temperature-controlled oven (GC4000, GL Sciences). The outlet of the generator column

100 was connected to a 1/8" stainless-steel trap column (2.2 mm i.d. × 0.4 m in length, GL

101 Sciences) and a Sep-Pak Plus PS-2 cartridge (Waters). The run times were 8–120 h,

102 depending on the oven temperature and the CP mixture composition. The nitrogen gas flow

103 was controlled at 1 mL min^{-1} with a mass flow controller (SEC-E40MK3 10SCCM, Horiba,

104 Kyoto, Japan) and the outflow was monitored using a mass flow meter to ensure no leak.

105 At a later time in the project, the flow was increased to 2 or 4 mL min^{-1} to measure low P

106 values. There was no significant influence of flow on the measured P values. The

107 temperature inside the oven was monitored using a quartz thermometer (DMT-600B,

108 Tokyo Dempa, Japan). The atmospheric pressure was measured using an MHB-382SD

109 portable barometer (MotherTool, Nagano, Japan). The trapped vapor sample was extracted

110 from the stainless-steel trap column using 10–20 mL acetone and from the Sep-pak

111 cartridge using 10 mL acetone. The extracts were evaporated to near dryness under a

112 nitrogen stream, after which 1 mL of methanol was added. The final extracts were

113 transferred to 1.5 mL HPLC vials for further analysis, as explained below. The extracts

114 from the Sep-pak cartridge did not contain an appreciable amount of CPs, confirming that

115 no breakthrough occurred in the stainless-steel trap column.

116   Vapor pressure measurements for Paroil 179-HV and Chlorowax 500C were performed

117 at 30, 40 and 50°C, and for SYCT-wax at 20, 30, 40 and 50°C. Experiments at 20°C were

118 only performed with the SYCT-wax mixture because of the low expected vapor pressures

119 that require an extensive time. For experiments performed at 20°C, the generator column

120 and the pre-heating column were submerged in a cooled water-bath instead of using the

121 temperature regulated oven. In some instances, experiments showed leaching of liquid CP

122 mixture from the generator column to the trap column. Leaching was identified from the

123 congener distribution pattern in the vapor sample that was similar to that of the original

124 mixture rather than would be expected in a vapor sample (i.e., high concentrations for most

125 abundant congeners in the mixture instead of most volatile congener groups). Results from

126 such experiments were not considered further.

127

128 *Quantification of CP congener groups in vapor samples*

129   An electrospray ionization−tandem mass spectrometer equipped with a liquid

130 chromatographic system (ACQUITY UPLC H-Class/Xevo TQ-S micro system; Waters

131 Corp., Milford, MA, USA) was used for the analysis. A ZORBAX SB-CN column (100

132 mm × 2.1 mm i.d., 1.8 μm; Agilent Technologies Inc.) was used for the separation of CP

133 congeners. A water solution containing 5 mM ammonium acetate was used as mobile phase

134 A and 100% methanol containing 5 mM ammonium acetate as mobile phase B. The

135 following gradient was used with minor modifications from the original parameters in our

136   earlier reports (Matsukami et al. 2020; McGrath et al. 2021): 0 min (60% B), 5 min (73%

137   B), 20 min (99% B), 22 min (99% B), and 22.1 min (60% B). For Chlorowax 500C and

138   SYCT-wax experiments, 25 SCCP congeners ($C_{10}Cl_{4-8}$, $C_{11}Cl_{4-9}$, $C_{12}Cl_{4-10}$, $C_{13}Cl_{4-10}$) and

139   28 MCCP congeners ($C_{14}Cl_{4-10}$, $C_{15}Cl_{4-10}$, $C_{16}Cl_{4-10}$, and $C_{17}Cl_{4-10}$) were quantified as

140   described previously   (Matsukami et al. 2020; McGrath et al. 2021). For Paroil 179-HV,

141   peak areas of 22 SCCP congeners, $C_{10}Cl_{7-11}$, $C_{11}Cl_{8-12}$, $C_{12}Cl_{8-13}$, and $C_{13}Cl_{9-14}$ were

142   acquired by the LC−ESI−MSMS method with optimization of multiple-reaction-monitoring

143   (MRM) transition parameters. Additional information with respect to MRM transitions for

144   the measurement of CP congeners is given in Tables S1−S3 of the Supplementary

145   Materials. The LOQ value was defined as a signal-to-noise ratio of 5 for the CP congeners

146   (Tables S4 and S5 of Supplementary Materials).

147

148   *Calculation of Vapor Pressure of CPs*

149   The partial vapor pressure (*P* in Pa) of each CP congener group was calculated from the

150   measured concentration using the ideal gas law:

151

152    $P = \frac{m}{MV_g} RT$ (1)

153

154   where *m* is the mass of the CP congener group measured in the vapor sample (g), *M* the

155   molar mass of the CP congener group (g mol^{-1}), *R* the gas constant, *T* the temperature (K)

156   inside the column oven and V_g the total volume of the carrier gas (L). V_g was obtained by

157   correcting the nominal gas volume, which is referenced to the standard condition, for the

158   actual pressure and temperature.

159   Raoult's law with the activity coefficient assumed to be 1 (eq 2) was used to convert the

160   measured P to the saturation vapor pressure (P^*):

161

162    $P^* = P/x$ (2)

163

164   where x is the mole fraction of the congener group of concern in the CP mixture. x was

165   derived as,

166

167    $x = w \dfrac{\overline{M_{mix}}}{M}$ (3)

168

169   w is the measured mass fraction of the congener group in the mixture. $\overline{M_{mix}}$ is the average

170   molar mass of the mixture (g mol^{-1}) and was estimated from the measured compositions of

171   the CP mixture. Here we consider each congener group as a pseudo-compound, bearing in

172   mind that actual P^* values differ across individual congeners.

173   Currently, there is no calibration standard available for the major congeners in the

174   highly chlorinated Paroil 179-HV mixture (e.g., $C_{10}Cl_9$, $C_{11}Cl_{10-11}$, $C_{12}Cl_{11-12}$ and $C_{13}Cl_{11-12}$

175    $_{12}$). Therefore, we determined P^* by using the peak areas of the CP congeners in the Paroil

176   179-HV mixture and vapor samples, as following. First, the mole fraction x of a CP

177   congener group in the Paroil 179-HV mixture can be expressed as,

178

179 $$x = \frac{\alpha PA_{mix}}{C_{mix,dilution}} \frac{\overline{M_{mix}}}{M} \tag{4}$$

180

181 where α is the response factor of the LC-ESI-MSMS analysis (g L^{-1} area counts^{-1}), PA_{mix}

182 the peak area from the analysis of diluted mixture solution (area counts), and $C_{mix,dilution}$ the

183 concentration of the mixture in the diluted solution that is injected to the LC (g L^{-1}). $\overline{M_{mix}}$

184 of Paroil 179-HV was estimated as 520 g mol^{-1}, based on the sum of molar masses of

185 congener groups weighted by their peak areas. P can be expressed as

186

187 $$P = \frac{\alpha PA_g V_{sol}}{M V_g} RT \tag{5}$$

188

189 where PA_g is the peak area from the analysis of the vapor sample (area counts), V_{sol} (L) the

190 final solution volume of the vapor sample that is subjected to the LC analysis (in our case 1

191 mL, see section *gas saturation method*) and V_g (L) is the volume of nitrogen carrier gas. By

192 inserting eqs 4 and 5 in eq 2, we can remove the unknown response factor (α) from the

193 equations and calculate P^* of the congener group:

194

195 $$P^* = \frac{P}{x} = \frac{PA_g}{PA_{mix}} \frac{V_{sol}}{V_g} \frac{C_{mix,dilution}}{\overline{M_{mix}}} RT \tag{6}$$

196

197 The assumption here is the activity coefficient being 1, as for eq 2.

198   The enthalpy of vaporization (ΔH_{vap}) was determined using the Clausius-Clapeyron

199   equation. Thus, ΔH_{vap} is derived from the slope of the logarithmic vapor pressure versus the

200   reciprocal temperature (eq 7).

201

202    $$\ln P^* = -\frac{\Delta H_{vap}}{R}\frac{1}{T} + c \tag{7}$$

203

204   where c is the regression constant.

205

206   *Prediction of Saturated Vapor Pressure by COSMO-RS-trained Fragment Contribution*

207   *Models (FCMs)*

208   COSMO-RS is a quantum chemically based prediction theory that can calculate

209   partition properties from molecular structure alone without the need for any empirical data.

210   In a recent publication, we presented a fragment contribution model (FCM) trained with the

211   COSMO-RS predictions as a tool to provide quantum chemically based COSMO-RS

212   predictions for partition coefficients of thousands of CP congeners within a short time

213   (Endo and Hammer 2020). In the continuation article (Endo 2021), the FCM was trained

214   for predicting log P^* and was used to calculate log P^* for thousands of congeners that likely

215   exist in CP technical mixtures. The median values of log P^* and ΔH_{vap} for each congener

216   group were taken from the article and compared to the experimental values from this work.

217

218

219

11

**RESULTS AND DISCUSSION**

Compositions of CP mixtures

Analysis of the CP technical mixtures showed that the SYCT-wax mixture consists of both SCCPs and MCCPs (C_{10}–C_{17}) with 4–10 Cl atoms per molecule, the Chlorowax 500C consists of SCCPs (C_{10}–C_{13}) with 4–10 Cl atoms per molecule, and the Paroil 179-HV mixture contains more chlorinated congeners and consists of SCCPs with 7–14 Cl per molecule, as shown in Figure S1A. Note that only the relative peak areas of measured congeners are presented for Paroil 179-HV.

Measured vapor pressures

Due to the low volatility at the applied temperatures, detected peak areas of congeners were comparatively small, particularly for the Paroil 179-HV mixture. The measured values of $\log P$ and $\log P^*$ are presented in Tables S6 to S10 and Figure S1. Obviously, distribution of the congeners in the vapor samples differed from that in the liquid mixture, as shorter and lower chlorinated congeners were more abundant in the vapor phase (see $\log P$ in Tables S6 and S7). Note, however, that $\log P$ values (thus, the amounts in the gas phase) of congener groups do not always decrease with increasing number of Cl atoms, as the abundance of low chlorinated congeners (e.g., Cl_4 congeners) can be low in the mixture (e.g., see $C_{11}Cl_4$ vs $C_{11}Cl_5$, Tables S6 and S7).

$\log P^*$ values at each temperature decreased with carbon chain length and with the number of Cl atoms (Figure 1). The widest variety of congener groups were measured at 50°C because of relatively high P and the data at this temperature are thus useful to

12

242   compare across the three mixtures. At 50°C, log P^* values of congener groups in SYCT-

243   wax and Chlorowax 500C were generally similar (see log P^* in Tables S8 to S10). Paroil

244   179-HV contains higher chlorinated congeners and their log P^* data were lower, in line

245   with the trend of the other two mixtures. Log P^* values of congener groups that were found

246   in all mixtures (i.e., $C_{10}Cl_7$ and $C_{11}Cl_8$) were within 0.5 log units between the three

247   mixtures (Figure 1). These results suggest that log P^* of a given congener group is largely

248   independent of the mixtures.

249
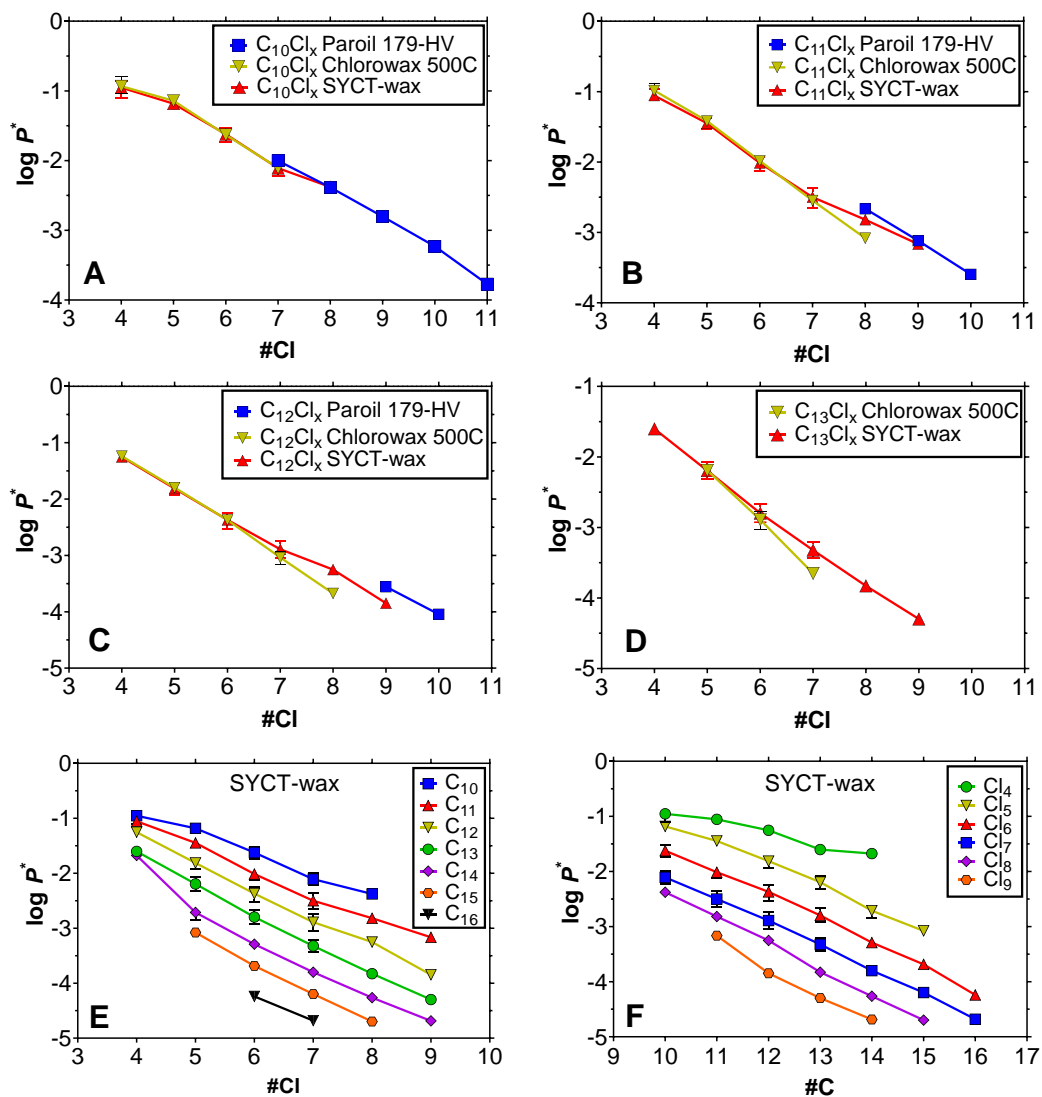
Figure 1. Log P^* values measured at 50°C for C_{10-13} congeners in the SYCT-wax,

Chlorowax 500C and Paroil 179-HV mixtures versus the number of Cl atoms (A−D), and

log P^* values at 50°C of all C_{10-16} congeners measured in the SYCT-wax mixture versus

number of Cl atoms (E) and the number of C atoms (F). Error bars indicate minimum and

maximum values.

255 *Temperature dependence of P^**

256   While we conducted the measurement of P from 20 to 50°C, data for 20°C are often

257 unavailable because of too low P. The temperature dependence thus has to be considered to

258 extrapolate P^* values at reference temperature of 25°C ($P^*_{25°C}$) or at environmental

259 temperature which can be even lower.

260   As expected, a linear relationship was found between log P^* and the reciprocal

261 temperature (Figure S2-4). The enthalpy of vaporization (ΔH_{vap}) was calculated using eq 7

262 (Table 1). ΔH_{vap} values were between 73 and 122 kJ mol^{-1} for $C_{10-14}Cl_{4-8}$ and are similar to

263 those found for polychlorinated biphenyls (PCBs) with similar degree of chlorination (Puri

264 et al. 2001; Nakajoh et al. 2006). The ΔH_{vap} values are somewhat higher than the values

265 estimated for CPs by Drouillard et al. using a GC retention method (67.3–92.5 kJ mol^{-1} for

266 $C_{10-12}Cl_{2-6}$) (Drouillard et al. 1998). The difference may be due to the different experimental

267 methods and/or different congener groups considered in the two studies. The ΔH_{vap} values

268 measured in this work seem to be similar between congener groups and there is no trend

269 with respect to the number of C or Cl atoms. Drouillard's data showed a slight increase in

270 ΔH_{vap} with increasing number of C atoms (~3 kJ mol-1) and Cl atoms (~5 kJ mol^{-1} per Cl).

271 The lack of a relationship in the current study may have resulted from the experimental

272 accuracy that was not high enough to detect such subtle differece in ΔH_{vap} between

273 congener groups (see the standard errors for the ΔH_{vap} data in Table 1). Particularly, P at

274 low temperatures were close to the limit of quantification but do affect the slope of the ln P

275 versus $1/T$ plot.

276   The ΔH_{vap} values predicted by the COSMO-RS-trained FCM were 80–120 kJ mol^{-1} for

277    $C_{10-14}Cl_{4-8}$ and in agreement with our experimental data (Table S11). In contrast to the

278   experimental data, the calculated ΔH_{vap} values from the COSMO-RS FCM show a positive

279   relationship between ΔH_{vap} and the number of C or Cl atoms. Predicted values of ΔH_{vap}

280   increase by ~5.5 kJ mol^{-1} per C atom and ~4.5 kJ mol^{-1} per Cl atom. All in all, the available

281   data suggest that ΔH_{vap} of $C_{10-14}Cl_{4-8}$ congener groups are ca 100 ± 20 kJ mol^{-1}. There may

282   be some positive dependence on the numbers of C and Cl atoms, which however needs to

283   be investigated further.

284

285

286

287

288

289

290

291

292

293

294

295

Table 1. Log $P^*_{25°C}$ values from inter- or extrapolation of experimental data for SYCT-wax,

log P^*_{MLR} values for 25°C using eq 8, and ΔH_{vap} values from experimental data for SYCT-

wax. P^* is in Pa.

Congener group	log $P^*_{25°C}$ ± standard error	log P^*_{MLR}	ΔH_{vap} (kJ mol^{-1}) ± standard error
$C_{10}Cl_4$	-2.14 ±0.21	-1.94	79 ±12
$C_{10}Cl_5$	-2.53 ±0.12	-2.44	99 ±5
$C_{10}Cl_6$	-3.01 ±0.07	-2.93	104 ±3
$C_{10}Cl_7$	-3.45 ±0.07	-3.43	101 ±4
$C_{11}Cl_4$	-2.33 ±0.15	-2.34	92 ±8
$C_{11}Cl_5$	-2.83 ±0.08	-2.83	102 ±3
$C_{11}Cl_6$	-3.40 ±0.07	-3.33	104 ±3
$C_{11}Cl_7$	-3.84 ±0.09	-3.82	101 ±4
$C_{11}Cl_8$	-4.20 ±0.12	-4.32	95 ±12
$C_{12}Cl_4$	-2.89 ±0.06	-2.73	122 ±6
$C_{12}Cl_5$	-3.23 ±0.07	-3.23	107 ±3
$C_{12}Cl_6$	-3.73 ±0.08	-3.73	102 ±3
$C_{12}Cl_7$	-4.18 ±0.09	-4.22	96 ±4
$C_{12}Cl_8$	-4.52 ±0.12	-4.72	84 ±9
$C_{13}Cl_5$	-3.54 ±0.08	-3.63	100 ±5
$C_{13}Cl_6$	-4.11 ±0.08	-4.12	98 ±4
$C_{13}Cl_7$	-4.52 ±0.1	-4.62	89 ±5
$C_{14}Cl_5$	-3.70 ±0.15	-4.02	73 ±9
$C_{14}Cl_6$	-4.43 ±0.14	-4.52	84 ±12
$C_{14}Cl_7$	-5.02 ±0.19	-5.02	94 ±17

P^* of CP congeners at 25°C and evaluation of prediction models

Measured log P^* values were used to inter- or extrapolate the values of log $P^*_{25°C}$. This

calculation was only performed for congener groups with measured vapor pressures at three

or more temperatures (Table 1). These experimentally based log $P^*_{25°C}$ values of CPs are

304   comparable to measured log P^* values of other semi-volatile persistent organic chemicals

305   such as PCBs at the same temperature and with the same number of Cl (−4.02 to −1.89 for

306   PCBs with Cl$_{4-7}$) (Lei et al. 2004; Nakajoh et al. 2006). Values of log $P^*_{25°C}$ are

307   furthermore well in line with experimental values from Drouillard et al. (Figure S5). Note

308   that experimental log P^* values from Drouillard et al. were derived from GC retention

309   measurements using reference compounds for which log P^* at 25°C was known. When

310   plotting both experimentally derived datasets against the number of Cl atoms, a nonlinear

311   relationship was observed. Thus, the vapor pressure seems to decrease more from 2 to 4 Cl

312   atoms than from 6 to 8 Cl atoms (Figure S5).

313   Using the vapor pressure data from the current study, a multiple linear regression

314   (MLR) model was developed to predict log P^* (log P^*_{MLR}). The model was set up with the

315   number of C atoms (#C), the number of Cl atoms (#Cl) and the reciprocal temperature (1/T)

316   in K^{-1} as independent variables. Using measured log P^* values for the SYCT-wax mixture

317   from 20 to 50°C as training data, we obtained:

318

319    $\log P^*_{MLR} = -0.397(\pm 0.005)\ \#C - 0.496(\pm 0.005)\ \#Cl - 5200(\pm 72)\ (1/T) + 21.46(\pm 0.26)$ (8)

320    $R^2 = 0.98$, SD $= 0.12$, $n = 312$

321

322   Here, we considered all replicate measurements as individual data. The congener

323   groups covered are $C_{10}Cl_{5-8}$, $C_{11-13}Cl_{4-9}$, $C_{14}Cl_{5-9}$, $C_{15}Cl_{5-8}$, and $C_{16}Cl_{6-7}$. This approach

324   assumes the same temperature dependence for all congener groups, following the

325   observations of ΔH_{vap} as presented above. In the calibration of the model, congeners $C_{10}Cl_4$

326   and $C_{14}Cl_4$ were excluded from the model input as these were clear outliers. This might be

327   related to the low sensitivity of the mass spectrometer for Cl_4 congeners, although the data

328   used were above an S/N ratio of 5. The measured log P^* values and the fitted values are

329   shown in Figure 2. The model fits the experimental vapor pressures for CP congeners well

330   with an R^2 of 0.98. The model predicts a 2.5-fold decrease in P^* with the addition of a C

331   atom and a 3.1-fold decrease in P^* with the addition of a Cl atom. The coefficient for $1/T$ (–

332   5200) corresponds to ΔH_{vap} of 101 kJ mol^{-1}, agreeing with the discussion in the previous

333   section.

334   The regression model from the current study (eq 8) shows a similar decrease in log P^*

335   with carbon chain length as compared to the regression model by Drouillard et al. (1998) (–

336   0.397 vs –0.353) for CP congener groups. In contrast, the decrease in log P^* with a Cl atom

337   is smaller in eq 8 than in Drouillard's model (–0.496 vs –0.645). This difference comes

338   from the fact that the dependence of log P^* on #Cl is not fully linear over a wide range of

339   #Cl, as previously discussed and shown in Figure S5. The training data of the current study

340   consisted of CP congeners with $Cl_{4–9}$ whereas the Drouillard's study included n-alkanes

341   and CP congeners with $Cl_{2–6}$. Thus, the current study considered higher chlorinated

342   congeners, for which log P^* is slightly less sensitive to #Cl, than in the literature study.

343   Both models can predict the experimentally derived log P^*_{25C} data well (Figure 3).

344   Predictions by Drouillard's model appear to be less accurate for higher chlorinated

345   congeners (i.e., Cl_8), consistent with the expectation from the model calibration set. The

346   new model (eq 8) is expected to have a larger domain of applicability than the literature

347   model, as eq 8 has been calibrated with directly measured data for more congener groups

348   and more temperatures, yet this expectation remains to be evaluated with external data.

349   Earlier than the development of COSMO-RS-trained FCMs, Glüge et al. (2013)

350   calculated log P^* values at 25°C using COSMO-RS for a selection of four structural

351   isomers per congener group, providing the maximum and minimum out of the four log P^*

352   values. In Figure 3B, the ranges of Glüge's predicted log P^* values are compared with the

353   experimentally based log $P^*_{25°C}$. While experimental data are within the ranges provided by

354   Glüge et al., log $P^*_{25°C}$ data for CPs with C_{10} and C_{11} tended to be at the lower limit and log

355    $P^*_{25°C}$ for CPs with C_{12} to C_{14} at the upper limit of predictions. Note that the ranges in

356   predicted log P^* values are large (e.g., more than 3 log units for $C_{13}Cl_7$) and increase with

357   the addition of C and Cl atoms to the CP congener groups.

358   A comparison of the experimentally based log $P^*_{25°C}$ data with the COSMO-RS-trained

359   FCM predictions is shown in Figure 3C. The median value of FCM predictions for a given

360   congener group agrees well with the experimental log $P^*_{25°C}$ ($R^2 = 0.96$; RSME = 0.25),

361   indicating high accuracy of FCM predictions.

362   Equation 8 was applied to predict the measured log P^* values from the Paroil 179-HV

363   mixture, which includes higher chlorinated congeners (Figure S6). Due to the low vapor

364   pressure of CP congeners in this mixture, most of the data were measured at 40 or 50°C

365   (Table S10). Generally, the model predictions for different temperatures agreed (RMSE =

366   0.25 log units) and correlated ($R^2 = 0.98$) well with the measured log P^*. However, the

367   calculated log P^*_{MLR} values are consistently lower than the measured data for these CPs,

368   which likely resulted from the model extrapolation and the inherent nonlinearity of log P^*

20

369 to #Cl. The COSMO-RS-trained FCM model predicted log P^* values that also agreed well

370 with the experimental log P^* values for the Paroil 179-HV mixture ($R^2 = 0.94$; RSME =

371 0.30) (Figures S6). For now, quantum-chemically based predictions may be used to fill

372 further data gaps, as they do not depend on the empirical calibration and can capture

373 nonlinear relationships between log P^* and structural features (see Figure S5).

374
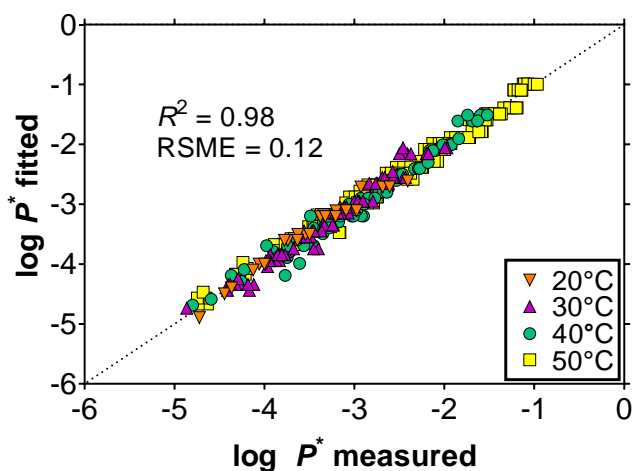
375

376 Figure 2. Calculated log P^* values with eq 8 versus measured data.

377
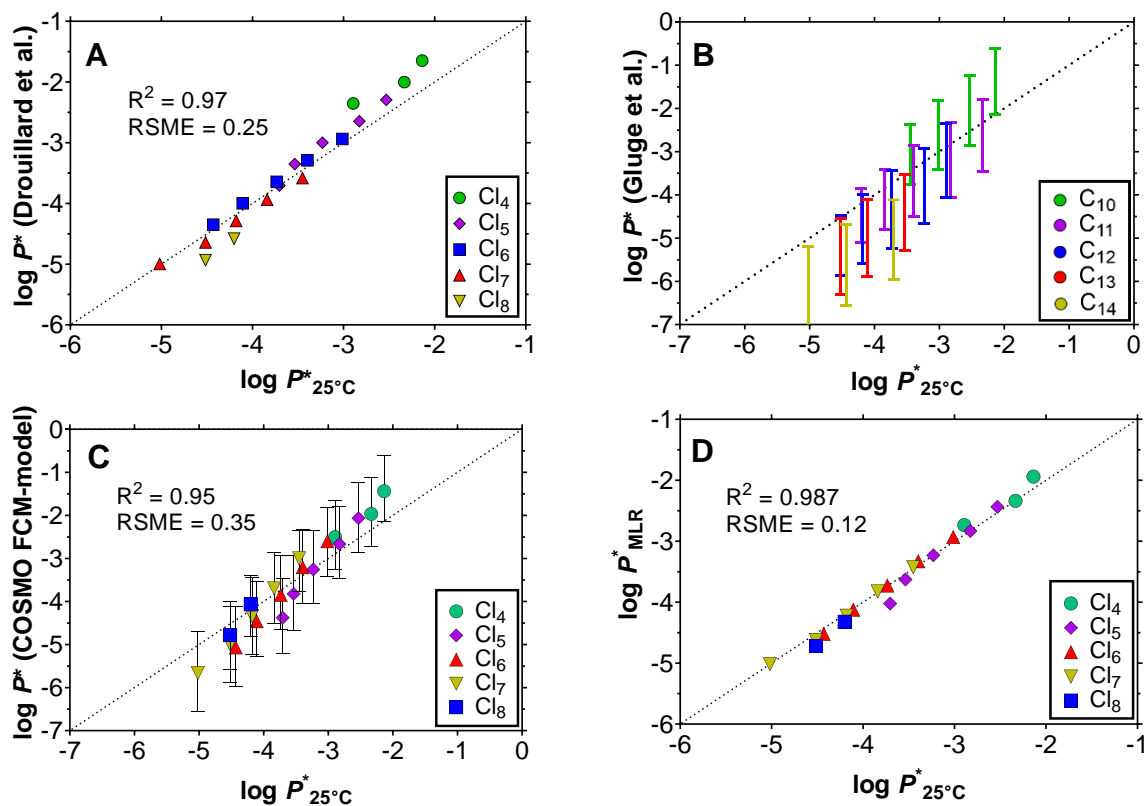
Figure 3. Comparison of experimentally-based log $P^*_{25°C}$ values with calculated vapor pressure data from the regression model by Drouillard et al. (1998) (A), from COSMO-RS calculations by Glüge et al. (2013) (B), from the COSMO-RS-trained FCM by Endo (2021) (C), and from eq 8 in the current study (D).

Comparing log P^* with gas/particle partitioning

The gas/particle partition coefficient (K_p) is a key parameter in determining the atmospheric transport and environmental fate of semi-volatile organic compounds (SVOCs), and the saturated vapor pressure has been used to model K_p of SVOCs (Pankow 1994; Lei et al. 2004). There are a few studies that presented environmental vapor

389   partitioning data for CPs: Ma et al. (2014) and Jiang et al. (2021) presented gas/particle

390   coefficients (K_p) derived from measured gas and particulate concentrations of CP congeners

391   in the Arctic region. Wang et al. (2012) measured concentrations of CPs in the atmosphere

392   of the Beijing area in summer and winter. Some of these published articles made only the

393   data for particulate fractions ϕ instead of K_p available. In those cases, we calculated

394    $\phi/(1-\phi)$, which is proportional to K_p. Moreover, Wang et al. (2015) measured vegetation/air

395   partitioning coefficients (C_v/C_p) by measuring CP concentrations in conifer needles. These

396   data are also related to volatility and are thus considered here. All literature data considered

397   are summarized in Table S12. We compared log P^* from the current and other studies to the

398   environmental partitioning data from the field studies cited above. Octanol/air partition

399   coefficients (K_{oa}) predicted by COSMO-RS-trained FCMs and EPISuite were also included

400   in the comparison. The comparison shows that R^2 is similar no matter which predictive

401   models are used and which of log P^* or log K_{oa} is considered. The new model (eq 8) shows

402   comparable results with existing models for CPs in terms of correlations with the field

403   partitioning data available in the literature. Note that only a few data points related to

404   volatility of MCCPs are available in the literature (e.g., only 2 MCCP congeners in Jiang's

405   data set and 5 in Ma's data set, see Table S4), and no data can be found for congeners with

406   more than 10 Cl atoms. Suitability of the models needs to be re-evaluated when data for

407   more congeners become available.

408

409

Table 2. Correlations (R^2) between the log of field-measured partition coefficients and

model-predicted $\log P^*$ or $\log K_{oa}$ values.

Sampling location (year)	Parameter	Current study $\log P^*_{MLR}$	Drouillard et al.,[e] $\log P^*$	Endo,[f] $\log P^*$	Endo,[f] $\log K_{oa}$	EPIsuite,[g] $\log K_{oa}$
Antarctic region (2013)[a]	$\log (\phi/(1-\phi))$	0.48	0.51	0.39	0.44	0.51
Antarctic region (2014)[b]	$\log K_p$	0.81	0.78	0.82	0.82	0.79
Antarctic region (2015)[b]	$\log K_p$	0.43	0.44	0.41	0.42	0.44
Antarctic region (2016)[b]	$\log K_p$	0.71	0.73	0.64	0.68	0.73
Antarctic region (2017)[b]	$\log K_p$	0.78	0.82	0.70	0.74	0.81
Antarctic region (2018)[b]	$\log K_p$	0.91	0.91	0.86	0.89	0.91
Beijing area in winter [c]	$\log (\phi/(1-\phi))$	0.84	0.83	0.78	0.81	0.83
Beijing area in summer [c]	$\log (\phi/(1-\phi))$	0.24	0.14	0.33	0.28	0.16
Beijing area [d]	$\log (C_v/C_g)$	0.77	0.77	0.79	0.82	0.70

[a] (Ma et al. 2014); [b] (Jiang et al. 2021); [c] (Wang et al. 2012); [d] (Wang et al. 2015); [e](Drouillard et al. 1998);

[f](Endo 2021); [g](EPA 2009)

Conclusions

In this work, for the first time, direct measurements of $\log P$ and $\log P^*$ for a broad

range of CP congener groups were performed using a gas saturation method. Log P^* of CPs

is found to be comparable to other POPs such as PCBs. A new model was calibrated and

validated with the newly measured data and can be used to estimate $\log P^*$ for a broad

range of CP congener groups. Note, however, that data for CP congener groups with more

than 10 Cl atoms are still limited. While the current study was able to measure $\log P^*$

values for CP congener groups in the highly chlorinated Paroil 179-HV mixture at 40 and

50°C, P^* for congeners in this mixture was too low to measure at ambient temperature by

the method used. Moreover, the absence of available calibration standards for such highly

chlorinated congeners did not allow us to determine the absolute values of P even at high

426 temperature. Extrapolation of the linear regression models presented here or elsewhere to

427 highly chlorinated congeners may cause additional errors, because of the nonlinear

428 relationship between $\log P^*$ and the number of Cl atoms. As a future work, vapor pressures

429 of these highly chlorinated CP congener groups should be investigated. Experimental data

430 are also limited for MCCPs and are totally absent for LCCPs, which also warrants further

431 studies.

432

440

441 *Disclaimer*

442 The authors declare no competing financial interest.

443

444 *Data availability*

445 The authors declare that all data supporting the findings of this study are available within

446 the article and its supplementary information file.

447

448   *Author Contributions statement*

449   Study design: JH, SE, HK. Gas saturation experiments: JH. LC/MS measurements: HM.

450   COSMO-RS calculations: SE. Data evaluation: JH, SE. Drafting of manuscript: JH.

451   Revising of manuscript: JH, SE, HM, HK.

452

453

454

455 **REFERENCES**

456 Brandsma SH, Brits M, Groenewoud QR, van Velzen MJM, Leonards PEG, de Boer J.

457 2019. Chlorinated Paraffins in Car Tires Recycled to Rubber Granulates and Playground

458 Tiles. Environ Sci Technol. 53(13):7595–7603. doi:10.1021/acs.est.9b01835.

459 Brandsma SH, van Mourik L, O'Brien JW, Eaglesham G, Leonards PEG, de Boer J, Gallen

460 C, Mueller J, Gaus C, Bogdal C. 2017. Medium-Chain Chlorinated Paraffins (CPs)

461 Dominate in Australian Sewage Sludge. Environ Sci Technol. 51(6):3364–3372.

462 doi:10.1021/acs.est.6b05318.

463 Drouillard KG, Tomy GT, Muir DCG, Friesen KJ. 1998. Volatility of chlorinated n-alkanes

464 (C10-C12): Vapor pressures and Henry's law constants. Environ Toxicol Chem.

465 17(7):1252–1260. doi:10.1002/etc.5620170709.

466 Endo S. 2021. Refinement and extension of COSMO-RS-trained fragment contribution

467 models for predicting partition properties of C10–20 chlorinated paraffin congeners.

468 doi:Submitted, in review. Preprint available at

469 https://doi.org/10.26434/chemrxiv.14256599.v1.

470 Endo S, Hammer J. 2020. Predicting partition coefficients of short-chain chlorinated

471 paraffin congeners by COSMO-RS-trained fragment contribution models. Environ Sci

472 Technol. 54(23):15162–15169. doi:10.1021/acs.est.0c06506.

473 Fridén UE, McLachlan MS, Berger U. 2011. Chlorinated paraffins in indoor air and dust:

474 Concentrations, congener patterns, and human exposure. Environ Int. 37(7):1169–1174.

475 doi:10.1016/j.envint.2011.04.002.

476 Glüge J, Bogdal C, Scheringer M, Buser AM, Hungerbühler K. 2013. Calculation of

477 Physicochemical Properties for Short- and Medium-Chain Chlorinated Paraffins. J Phys

478 Chem Ref Data. 42(2):023103. doi:10.1063/1.4802693.

479   Hammer J, Matsukami H, Endo S. 2020. Congener-specific partition properties of

480   chlorinated paraffins evaluated with COSMOtherm and GC-retention indices. Sci Rep.

481   11(1):4426. doi:10.1038/s41598-021-84040-z.

482   Hilger B, Fromme H, Völkel W, Coelhan M. 2011. Effects of chain length, chlorination

483   degree, and structure on the octanol-water partition coefficients of polychlorinated n-

484   alkanes. Environ Sci Technol. 45(7):2842–2849. doi:10.1021/es103098b.

485   Huang H, Gao L, Xia D, Qiao L, Wang R, Su G, Liu W, Liu G, Zheng M. 2017.

486   Characterization of short- and medium-chain chlorinated paraffins in outdoor/indoor PM 10

487   /PM 2.5 /PM 1.0 in Beijing, China. Environ Pollut. 225:674–680.

488   doi:10.1016/j.envpol.2017.03.054.

489   Jiang L, Gao W, Ma X, Wang Yingjun, Wang C, Li Y, Yang R, Fu J, Shi J, Zhang Q, et al.

490   2021. Long-Term Investigation of the Temporal Trends and Gas/Particle Partitioning of

491   Short- and Medium-Chain Chlorinated Paraffins in Ambient Air of King George Island,

492   Antarctica. Environ Sci Technol. 55(1):230–239. doi:10.1021/acs.est.0c05964.

493   Kuramochi H, Takigami H, Scheringer M, Sakai SI. 2014. Measurement of vapor pressures

494   of selected PBDEs, hexabromobenzene, and 1,2-bis(2,4,6-tribromophenoxy)ethane at

495   elevated temperatures. J Chem Eng Data. 59(1):8–15. doi:10.1021/je400520e.

496   Lei YD, Wania F, Mathers D, Mabury SA. 2004. Determination of Vapor Pressures,

497   Octanol−Air, and Water−Air Partition Coefficients for Polyfluorinated Sulfonamide,

498   Sulfonamidoethanols, and Telomer Alcohols. J Chem Eng Data. 49(4):1013–1022.

499   doi:10.1021/je049949h.

500   Ma X, Zhang H, Zhou H, Na G, Wang Z, Chen C, Chen Jingwen, Chen Jiping. 2014.

501   Occurrence and gas/particle partitioning of short- and medium-chain chlorinated paraffins

502   in the atmosphere of Fildes Peninsula of Antarctica. Atmos Environ. 90:10–15.

503   doi:10.1016/j.atmosenv.2014.03.021.

504 Matsukami H, Kajiwara N. 2019. Destruction behavior of short- and medium-chain
505 chlorinated paraffins in solid waste at a pilot-scale incinerator. Chemosphere. 230:164–172.
506 doi:10.1016/j.chemosphere.2019.05.048.

507 Matsukami H, Takemori H, Takasuga T, Kuramochi H, Kajiwara N. 2020. Liquid
508 chromatography–electrospray ionization-tandem mass spectrometry for the determination
509 of short-chain chlorinated paraffins in mixed plastic wastes. Chemosphere. 244:125531.
510 doi:10.1016/j.chemosphere.2019.125531.

511 McGrath TJ, Poma G, Matsukami H, Malarvannan G, Kajiwara N, Covaci A. 2021. Short-
512 and Medium-Chain Chlorinated Paraffins in Polyvinylchloride and Rubber Consumer
513 Products and Toys Purchased on the Belgian Market. Int J Environ Res Public Health.
514 18(3):1069. doi:10.3390/ijerph18031069.

515 van Mourik LM, Wang X, Paxman C, Leonards PEG, Wania F, de Boer J, Mueller JF.
516 2020. Spatial variation of short- and medium-chain chlorinated paraffins in ambient air
517 across Australia. Environ Pollut. 261:114141. doi:10.1016/j.envpol.2020.114141.

518 Nakajoh K, Shibata E, Todoroki T, Ohara A, Nishizawa K, Nakamura T. 2006.
519 Measurement of temperature dependence for the vapor pressures of twenty-six
520 polychlorinated biphenyl congeners in commercial Kanechlor mixtures by the Knudsen
521 effusion method. Environ Toxicol Chem. 25(2):327–336. doi:10.1897/05-215R.1.

522 Nishida T, Fujimori T, Eguchi A, Takaoka M. 2019. Characteristics of high-temperature-
523 induced destruction of short-chain chlorinated paraffins in wax. 39th Int Symp Halogenated
524 Persistent Org Pollut. 81:383–386.

525 Pankow JF. 1994. An absorption model of the gas/aerosol partitioning involved in the
526 formation of secondary organic aerosol. Athmospheric Environ. 28(2):189–193.
527 doi:10.1016/1352-2310(94)90094-9.

528   Puri S, Chickos JS, Welsh WJ. 2001. Determination of Vaporization Enthalpies of

529   Polychlorinated Biphenyls by Correlation Gas Chromatography. Anal Chem. 73(7):1480–

530   1484. doi:10.1021/ac001246p.

531   Sverko E, Tomy GT, Märvin CH, Muir DCG. 2012. Improving the quality of

532   environmental measurements on short chain chlorinated paraffins to support global

533   regulatory efforts. Environ Sci Technol. 46(9):4697–4698. doi:10.1021/es301390v.

534   Tomy GT, Fisk AT, Westmore JB, Muir DCG. 1998. Environmental chemistry and

535   toxicology of polychlorinated n-alkanes. Rev Environ Contam Toxicol. 158:53–128.

536   doi:10.1007/978-1-4612-1708-4_2.

537   United Nations Environment Programme (UNEP). 2017. UNEP/POPS/COP.8/SC-8/11.

538   Listing of short-chain chlorinated paraffins.

539   Wang T, Han S, Yuan B, Zeng L, Li Y, Wang Y, Jiang G. 2012. Summer-winter

540   concentrations and gas-particle partitioning of short chain chlorinated paraffins in the

541   atmosphere of an urban setting. Environ Pollut.(171):38–45.

542   doi:10.1016/j.envpol.2012.07.025.

543   Wang T, Yu J, Han S, Wang Y, Jiang G. 2015. Levels of short chain chlorinated paraffins

544   in pine needles and bark and their vegetation-air partitioning in urban areas. Environ Pollut.

545   196:309–312. doi:10.1016/j.envpol.2014.10.025.

546   Widegren JA, Bruno TJ. 2010. Gas saturation vapor pressure measurements of

547   mononitrotoluene isomers from (283.15 to 313.15) K. J Chem Eng Data. 55(1):159–164.

548   doi:10.1021/je900293j.